Perceptual Evaluation of Steered Retinal Projection

Seungjae Lee*
Meta
United States of America
seungjae@meta.com

Seung-Woo Nam*
Meta
United States of America
711asd@snu.ac.kr

Kevin Rio
Meta
United States of America
kevinwrio@meta.com

Renate Landig
Meta
United States of America
landig@meta.com

Hsien-Hui Cheng
Meta
United States of America
hsienhuicheng@meta.com

Lu Lu
Meta
United States of America
llu@meta.com

Barry Silverstein
Meta
United States of America
bsilverstein@meta.com

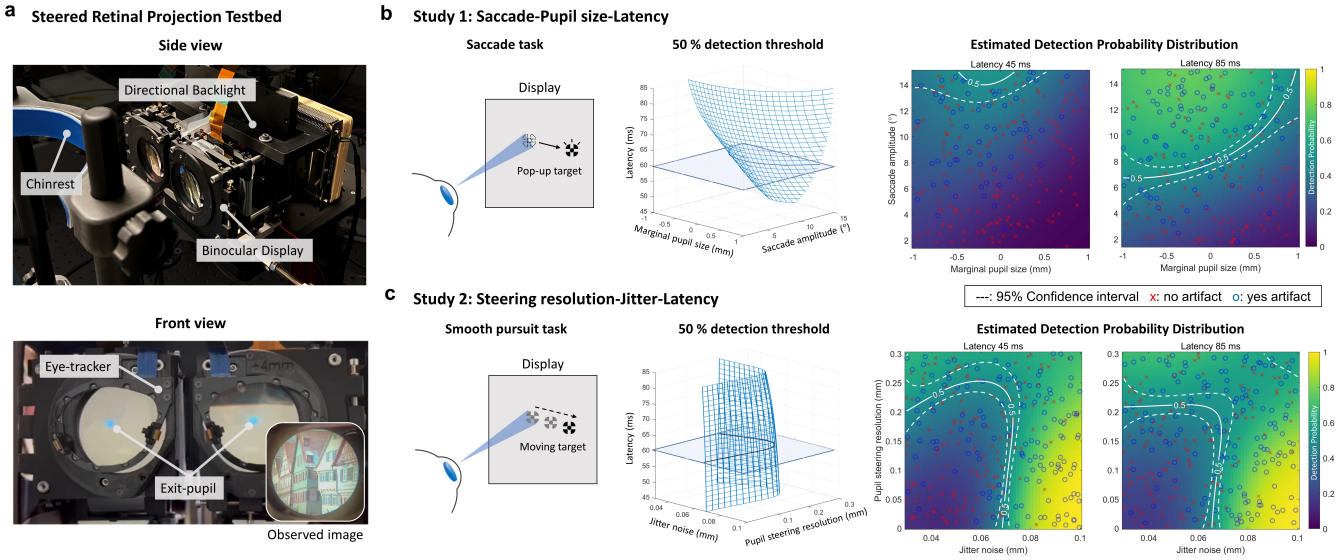

Figure 1: (a) Steered retinal projection (SRP) testbed to conduct fundamental studies to evaluate the perceptual experience for the dynamic pupil steering. The testbed consists of directional backlight, binocular display, and a chinrest to deliver the pupil steering experience to a user. The directional backlight formulates a small exit-pupil as demonstrated in the front-view, and steers the exit-pupil to the eye-pupil position estimated by an eye-tracker. (b-c) We conducted two independent user study sessions to investigate 3D trade spaces for different eye movement dynamics of saccade and smooth pursuit. We collected responses from 9 subjects whether they recognized a visual artifact during each trial, and merged data points to fit a detection probability model [Owen et al. 2021]. The first and second studies explored the trade space among saccade amplitude, exit-pupil diameter, and steering latency, and steering resolution, jitter, and latency, respectively. The right-most figures illustrate 50% detection thresholds and detection probability distribution for each trade space.

ABSTRACT

Steered retinal projection (SRP) is an emerging display technology that combines retinal projection and pupil steering to achieve exceptional light efficiency and a consistent viewing experience. Retinal projection enables most photons from a display projector to

*Both authors contributed equally to this research.

SIGGRAPH Conference Papers '24, July 27–August 01, 2024, Denver, CO, USA

ACM ISBN 979-8-4007-0525-0/24/07
https://doi.org/10.1145/3641519.3657486

reach the retina, and pupil steering dynamically aligns the narrow viewing window of the retinal projection with the eye. While SRP holds considerable promise, its development has been stagnant due to a lack of understanding how human vision reacts to the dynamic steering movement of the viewing window. To delve into these areas, this study introduces the first SRP system testbed specifically designed for perceptual studies on the viewing experience of pupil steering. The testbed replicates the SRP viewing experience and offers the flexibility in adjusting several parameters including steering resolution, accuracy, and latency. We conducted two perceptual studies utilizing the testbed. The first study investigates the impact of saccadic suppression, a phenomenon that reduces visual sensitivity during rapid eye movements, on the SRP viewing experience. The second study explores the trade space between eye-tracking and pupil steering performance, providing insights into the optimal balance between these factors. Additionally, we introduce a numerical model to predict the detection probability for SRP artifacts considering the temporal characteristics of global luminance and the human vision system. This model enables a more comprehensive interpretation of user study and provides preliminary hardware requirements for SRP systems. The findings from this study offer invaluable research directions that may help determine component-level development milestones for SRP development, paving the way for the practical implementation of this promising technology.

CCS CONCEPTS

• **Computing methodologies → Perception**.

KEYWORDS

Pupil steering, Retinal projection

ACM Reference Format:

Seungjae Lee, Seung-Woo Nam, Kevin Rio, Renate Landig, Hsien-Hui Cheng, Lu Lu, and Barry Silverstein. 2024. Perceptual Evaluation of Steered Retinal Projection. In *Special Interest Group on Computer Graphics and Interactive Techniques Conference Conference Papers '24 (SIGGRAPH Conference Papers '24), July 27–August 01, 2024, Denver, CO, USA.* ACM, New York, NY, USA, 11 pages. https://doi.org/10.1145/3641519.3657486

1 INTRODUCTION

Steered retinal projection (SRP) is an advanced display technology that combines the principles of retinal projection and pupil steering. The display technology called retinal projection guides photons from a display module into a directional beam with a narrow exit-pupil (smaller than the eye-pupil). The directional beam is designed to pass through the eye-pupil and reach the retina with the image information [Westheimer 1966]. The pupil steering dynamically aligns the retinal projection's exit-pupil with the eye-pupil that has a natural movement in response to gaze direction [Jang et al. 2017; Kim et al. 2019]. With the eye-tracking, the pupil steering addresses a drawback of the retinal projection where viewers may experience partial or complete image loss [Cholewiak et al. 2020; Ratnam et al. 2019] if the pupils are misaligned. If the alignment of the projection's exit-pupil and the viewer's eye-pupil is guaranteed, SRP may deliver the image information without any loss of photons and achieve high efficiency. This attribute is particularly beneficial for the development of augmented reality (AR) devices where we often face challenges for power consumption and low brightness [LiKamWa et al. 2014].The potential advantages of SRP have spurred numerous research initiatives aimed at developing SRP systems for AR applications [Lin et al. 2017a].

Despite the potential advantages of SRP, creating a compelling prototype that outlines a promising development path for a product remains a significant challenge. Also, there is a lack of clarity regarding the ultimate milestones for component-level development and the distance to the goal from our state-of-the-art capability. A significant concern is the uncertainty surrounding the effectiveness of pupil steering, even if all components function as designed. This is due to the fact that SRP does not replicate a viewing experience that can be observed in nature, and there could be a substantial discrepancy between theoretical predictions and practical outcomes. The potential existence of unknown perceptual artifacts associated with SRP technologies further compounds this issue. This risk eventually hinders a long-term investment in research for component-level development to enable seamless pupil steering. The observation of the risk have motivated us to develop a perceptual testbed to investigate the pupil steering viewing experience, with the ultimate goal of providing perceptual requirements for SRP hardware development.

In this study, we demonstrate the first testbed for SRP system, specifically designed to conduct perceptual studies and evaluate the SRP viewing experience. The testbed imitates pupil steering and replicates the SRP viewing experience with lots of flexibility to modulate the system performance for the steering resolution, accuracy, and latency. The versatile capability of the testbed enables us to facilitate various perceptual studies. To the best of our knowledge, this is the first system that provides a real-life experience of pupil steering to users and enables us to evaluate its perceptual effectiveness of SRP system. Utilizing this testbed, we conducted two distinct perceptual studies to delve into the unexplored aspects of pupil steering and answer two research questions: 1) whether saccadic suppression [Stevenson et al. 1986] relaxes hardware requirements for seamless SRP viewing experience, and 2) how the trade space is formed between eye-tracking and pupil steering performance axes (e.g., pupil steering interval, latency, and jitter). The user study protocol for each research question was designed to stimulate an appropriate eye movement dynamic: saccade and smooth pursuit.

We also introduce a numerical model to predict the detection probability for the pupil steering. This model offers a more comprehensive interpretation of the user study results, which are not fully interpreted by with the previous model that only considered global transmittance [Ratnam et al. 2019]. Our model incorporates considerations of temporal frequency components of global luminance [Roufs 1972; Watson 1986], temporal contrast sensitivity [Robson 1966], and the saccadic suppression [Braun et al. 2017; Stevenson et al. 1986]. The model calculates visual stimuli intensity using Minkowski summation [To et al. 2011; Tursun and Didyk 2022], and predicts the detection probability of the artifacts through a psychometric function [Wichmann and Hill 2001]. This proposed model allows us to investigate further trade space that the testbed cannot reach due to the hardware limit. Furthermore, we may utilize the perceptual model to optimize the pupil steering strategies to relax the hardware requirements.

We will conclude this study with additional discussions on the preliminary hardware requirements of SRP, limitations of our studies, and the discovery of a visual artifact (which we term as 'ocular pupil swim') that could be observed only in the pupil steering system. The following are our research contributions.

- We implemented a perceptual testbed that enables proof-of-experience and perceptual studies for SRP system.
- We explored 3D trade spaces of SRP regarding two different eye movement dynamics: saccade and smooth pursuit.
- We formulated a numerical prediction model of artifact detection probability for SRP viewing experience.
- We found a unique visual artifact observed in pupil steering system due to the eye-pupil aberration.

2 RELATED WORK

Retinal Projection. Retinal projection displays, also recognized as Maxwellian-view displays, are defined as near-eye displays with an exit-pupil smaller than the eye-pupil [Kollin and Tidwell 1995; Lin et al. 2017a; Westheimer 1966]. The diminutive size of the exit-pupil has shown the advantages in increasing power efficiency and mitigating vergence-accommodation conflict [Hoffman et al. 2008; Konrad et al. 2017; Kramida 2016]. There have been several attempts to implement the retinal projection leveraging a display projector with a diffractive combiner [Jang et al. 2017], a metasurface [Song et al. 2023], a partially reflective mirror [Lin et al. 2017b; Zhang et al. 2020]. Holographic near-eye displays [Jang et al. 2018; Kim et al. 2022] are also considered a family of retinal projection as they have a narrow eye-box given by a combination of a reflective LC display panel and an engineered light source with a small numerical aperture.

Pupil Steering. The small exit-pupil inherent in retinal projection presents a limited tolerance for the eye movement, which should be addressed by pupil steering. Several methods have been presented for pupil steering, leveraging a motorized stage for the combiner adjustment [Kim et al. 2019], a MEMS mirror for display projection steering [Jang et al. 2018, 2017; Kim et al. 2022; Lee et al. 2020], or an angular multiplexed volume grating combiner [Kim and Park 2018]. Additionally, there was an attempt to apply polarization-dependent switching elements that may support discontinuous steering [Lee et al. 2020; Lin et al. 2020; Xiong et al. 2021; Zou et al. 2022]. However, there have been no specific criteria to evaluate these approaches and prioritize the most promising one for successful SRP development. This lack of evaluation criteria is primarily due to a limited understanding of the requirements for pupil steering.

Visual Perception in Display. The perceptual recognition of human vision is indeed complicated and influenced by display factors including luminance, field of view, eccentricity, and refresh rate [Krajancich et al. 2021; Krauskopf 1980; Mantiuk et al. 2022; Tursun and Didyk 2022; Watson 1986]. It is important to understand how human vision perceives displays to optimize the viewing experience. However, there are only a few comprehensive evaluations of SRP viewing experience. Some studies [Bradley et al. 1990; Cholewiak et al. 2020; Thibos et al. 1992; Van Meeteren and Dunnewold 1983] reported an image quality degradation of retinal projection due to the misalignment of pupils and spatially-varying aberrations of the eye-lens. Ratnam et al. [2019] have contributed to understanding SRP viewing experience by evaluating the perceptual image quality of images through geometric optical simulations. While this study could offer valuable analysis for the viewing experiences associated with various pupil steering scenarios, authors also highlighted further validation of their work is required through user studies.

It is often considered much more complicated and challenging to comprehend the recognition sensitivity especially when there is a dynamic eye movement [Idrees et al. 2020; Kelly 1979; Stevenson et al. 1986]. These challenges motivated several research efforts to revisit and analyze the human vision response for near-eye displays using eye-tracking technologies. Gaze-contingent displays [Chen et al. 2022; Duinkharjav et al. 2022b; Patney et al. 2016] have been evaluated through user studies where the display imagery is updated accordance of the eye movement. Guan et al. [2022] identified the detection threshold of the pupil swim artifacts observed in near-eye displays. Moreover, statistic analysis of the eye movements [Aizenman et al. 2023] and the relationship between visual stimuli and the behavior of the human eye [Duinkharjav et al. 2022a, 2023] further enriched our understanding of dynamic eye movements. As an extended effort, SRP development also requires perceptual studies to allow a more accurate reflection of real-world viewing experiences.

3 STEERED RETINAL PROJECTION TESTBED

Implementation of a testbed for perceptual studies is the first milestone towards understanding the visual perception aspects of pupil steering. The primary objective when designing the optical configuration of the testbed is to reproduce the pupil steering viewing experience for users. The flexibility of pupil steering specifications (e.g., steering resolution, latency, and jitter) is also crucial to expand the design space of perceptual study protocols.

3.1 Optical Configuration

The testbed must be capable of pupil steering at a reasonable speed and refresh rate. Additionally, pupil steering should minimally affect the pupil shape or viewing image of the display system. Among several candidates for pupil steering, we found the directional backlight configuration [Kim et al. 2022] to be the most promising approach to meet the qualifications. The directional backlight is a light source that can adjust the illumination direction for the display panel. When applied to an optical configuration for a virtual reality (VR) headset, it can be used for pupil steering. The illumination direction determines where the exit-pupil is formed, and the cone angle of the illumination corresponds to the exit-pupil diameter. In other words, we can steer the exit-pupil position and control the exit-pupil diameter with an appropriate modulation of the directional backlight. Another benefit of the directional backlight is that we can reuse the optical configuration used for commercially available VR headsets to deliver a display viewing experience.

The directional backlight can be built using a monochrome liquid crystal display (LCD) on an LED source, as shown in the Fig. 2. The relay optics collimates a diverging beam from the monochrome LCD, corresponding to the Fourier transform of the light emitting profile. The collimated beam direction is determined by the relative position

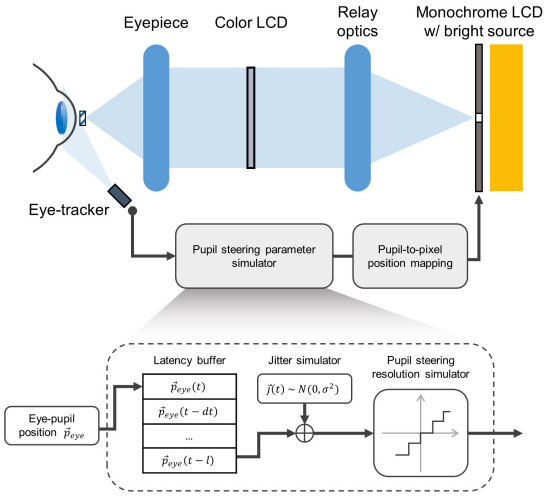

Figure 2: Illustration of the optical configuration of the SRP testbed. A combination of the light source, monochrome LCD, and relay optics enables a directional backlight unit to steer the exit-pupil of the color LCD display. The monochrome LCD is synchronized with an eye-tracker and steers the exit-pupil by adjusting transmissive area. The eye-tracker returns the eye-pupil position to the main processor, and the processor refreshes the monochrome LCD image. The main processor may apply additional processing to the eye-tracking's input to simulate variant latency, jitter, and steering resolution.

of light emission to the optical axis, and the cone angle is determined by the light emitting aperture. The directional backlight illuminates another color LCD panel, which displays the viewing imagery to users. The color LCD panel is then relayed by the viewing optics, following a general architecture of pancake optics for VR products. Note that the pancake optics architecture is known to reduce the pupil swim artifact [Guan et al. 2022] including the field of view shift or distortion. It is beneficial for our study as it can minimize artifacts involved solely by eye movement. We adopted an off-the-shelf pancake lens used for Quest Pro, but customized some lenses to further minimize the artifacts. The optical customization ensures that the visual perception of the SRP testbed is mostly affected by the pupil steering dynamics.

The other important hardware component of the testbed is an eye-tracker that measures the pupil position and feeds the information back to the backlight module for pupil steering. We integrated the eye-tracking system on top of the last surface of the viewing optics. We used a desktop PC as the main station for the data communications, which renders and refreshes the backlight LCD mask images according to the pupil positions as shown in Fig. 2. Note that the main station may apply additional signal processing to simulate variable pupil steering latency, jitter, and resolution. For instance, we intentionally referred a delayed buffer of the eye-tracking to simulate an SRP system with a longer pupil steering latency. The system operation is run by a Python environment, and a GPU is used for rendering to improve the display latency.

3.2 System Specifications

The system specifications of the SRP testbed are follows. The field of view is 50° in a circular shape, the display resolution is 12 ppd, the eye-relief is 18 mm, and the luminance is 50 cd/m^2. The exit-pupil can be steered to ±6 mm from the optical axis with the acuity of 0.14 deg and the refresh rate of 50 Hz. A linear stage is integrated to adjust the inter-pupillary distance (IPD) between 62-70 mm. The pupil swim magnitude of the eye-piece was minimized to 58 um at the display plane, which corresponds to the field of view shift of 0.13 degree for the saccade movement of 15 degree. The eye-tracking measures the eye-position at 240 Hz with a random noise that follows normal distribution with a standard deviation of 0.03 mm. The end-to-end latency, the time from the pupil movement to the pupil steering, is 45 ms.

4 USER STUDY DESIGN

Our goal for user study is to enable further understanding how human vision perceives the SRP viewing experience. To be more specific and narrow down our scope of the perceptual studies, we may consider two building blocks for the user study design. One is which research question we are trying to answer from the user study, and the other one is how we would stimulate participants to move their gaze direction. In this study, we determined two research questions to be explored.

4.1 Research Questions

The first research question is whether SRP can benefit from a phenomenon known as saccadic suppression, which is a reduction in visual sensitivity during rapid eye movements [Matin 1974; Stevenson et al. 1986]. If saccadic suppression can help reduce the likelihood of detecting SRP artifacts, it could greatly expand the range of potential solutions for pupil steering systems. This would be a key milestone for SRP development, especially considering that even a small misalignment of the pupil (0.5 mm) might be perceived as an artifact in a static environment [Ratnam et al. 2019]. If the same standard is applied for the dynamic condition, the misalignment tolerance corresponds to a minimal latency (5 ms) of the steering system for >15° saccades. It is indeed a challenging requirement for eye-tracking or steering devices to meet. Therefore, it is important to find ways to ease these hardware requirements for SRP, and saccadic suppression could be one such solution.

The second research question is how detection probability of the SRP artifact is determined by steering parameters such as steering resolution, latency, and jitter. Our goal is to learn insights for perceptual requirements to achieve seamless and consistent SRP viewing experience. Answering this question helps us to determine which pupil steering approaches are promising and feasible for SRP development in the long-term. For example, we may narrow down the candidates for steering components according to the steering resolution requirements. If quasi-continuous pupil steering is necessary, a scanning mirror would be more promising solution than

an electric switching device for binary steering. We can also confirm whether state-of-the-art eye-tracking device is good enough to support SRP system.

4.2 User Study Protocol

The user study protocol design should consider the eye movement dynamics that could affect the visual recognition characteristics. There are four categories of eye movements: saccade, smooth pursuit, vergence, and vestibulo-ocular reflex [Purves and Williams 2001]. Each study protocol aims to stimulate only one type of eye movement to isolate the control variable.

4.2.1 Study 1: Saccadic suppression in SRP experience. The Study 1 aims to explore the effect of saccadic suppression to the SRP viewing experience. Consequently, the Study 1 protocol was designed to stimulate saccade for various amplitudes. Other movements such as vergence or vestibulo-ocular reflex were minimized by using a 2D checkerboard image and a chinrest for minimal depth stimulation and head fixation, respectively. During the session for Study 1, a subject is instructed to look through the eyepiece of the SRP testbed and play a kind of whack-a-mole game. The protocol of the Study 1 is illustrated in Fig. 3(a). The subject will find a gaze marker that appears at a random location in a grid checkerboard with a white background. When the subject identifies where the marker is located and fixes their gaze at that point, the marker disappears and reappears simultaneously in a different location. The new location is randomly determined within the points separated by a specific saccade distance from the previous location. The whack-a-mole game repeats 3 times, and then the subject responses to a 'yes' or 'no' question of "artifact detected" by using a mouse (left click: 'yes' and right click: 'no'. After a short break (1 second) with a grey background, a single trial ends.

The subject takes around 200 trials, and each trial is run by different steering specifications. For each trial we randomly sample three different steering parameters: exit-pupil diameter, saccade amplitude, and steering latency. Exit-pupil diameter and steering latency are supplemented for additional control variables because they are also largely correlated with the pupil misalignment errors. We used a quasi-random sampling called Sobol sequence to ensure the sampling distribution is uniform across the exploration space. The sampling range of the saccade amplitude is between 1.5° and 15°, the exit-pupil diameter is +/- 1 mm of the subject's eye-pupil diameter, and the steering latency is set to 45 ms to 85 ms. Note that we determined the sampling range of each parameter after a few sessions of pilot studies and trimmed the sampling space into a specific area that showed critical points.

4.2.2 Study 2: Trade space exploration between resolution, latency, and jitter. Study 2 aims to explore the trade space for pupil steering between three parameters: steering resolution, latency, and jitter. The steering resolution represents the minimum step distance to which the exit-pupil can be steered, the latency is the response time of the steering system from eye movement, and jitter is random noise for pupil steering. These parameters were selected as they are closely related to hardware requirements for steering devices and eye-tracking systems. Note that the exit-pupil diameter was fixed to (eye-pupil diameter - 1 mm) and not included in the trade space exploration. We assumed that the exit-pupil diameter variation has minimal contributions to SRP artifacts for smooth pursuit movements as eye-pupil moves slowly.

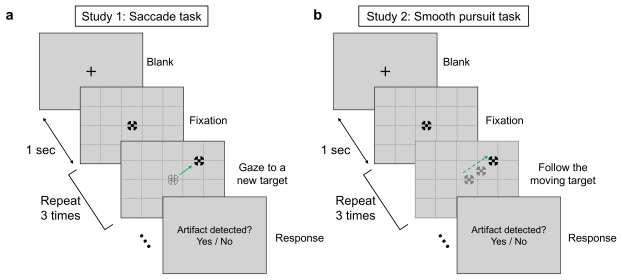

Figure 3: Schematic diagram of the user study protocol. The subjects are instructed to gaze at a marker during the session. Each trial starts with a blank scene featuring the gaze marker at the center, and ends with 'yes' or 'no' response of the subjects to the question of "artifact detected?". (a) In Study 1, the gaze marker disappears and reappears at a random location to stimulate saccade of a specific amplitude. (b) In Study 2, the gaze marker moves to a random location with a constant speed to stimulate smooth pursuit.

Study 2 also follows the same protocol of Study 1 except for the stimulus task. Study 2 designed a different task to stimulate smooth pursuit eye movement, allowing artifact detection to be independent to the saccade amplitude and saccadic suppression [Stevenson et al. 1986]. The schematic diagram of the task is illustrated in Fig. 3(b). Subjects were instructed to gaze at a specific marker that moves to an end point with a constant speed (10°/s). After reaching the end point, the marker paused for 1 second before moving to another random point. The SRP testbed simulates different steering specifications for each trial, and the sampling ranges for steering resolution, latency, and jitter are 0.01 mm to 0.3 mm, 45 ms to 85 ms, and 0.03 mm to 0.1 mm, respectively. The lower bound of each parameter was determined by the hardware limitations of the SRP testbed. Note that the other processes not mentioned are identical with Study 1.

4.2.3 Subjects and calibration. We invited nine subjects (six males, three females, aged 20-40) for the user study and they have normal vision with naked eyes or wearing contact lenses. All subjects participated in both Study 1 and Study 2 in a single or separate days. The subjects were instructed to place their head on a chinrest and find the comfortable position during the session. Prior to the session, the subjects calibrated their gaze with the eye-tracker. We measured the eye-pupil diameter and the IPD of the subjects using the eye-tracker.

The subjects underwent a training process at the beginning of Study 1 and Study 2. As a reference viewing experience without artifact, the SRP testbed with large exit-pupil (12 mm diameter) was provided. We also presented the worst viewing condition of the SRP testbed that might be seen during the session. This process guides the subject to understand the artifacts arising from pupil steering.

5 RESULTS

The responses of the nine subjects were consolidated into a single model using adaptive experimentation for human perception and perceptually-informed outcomes (AEPsych) [Owen et al. 2021] to visualize the average trend of the user responses. AEPsych fits the merged data into a nonparametric model that provides the detection probability of artifacts across the control variable axes. This tool is particularly efficient when exploring a trade space with more than two axes, as it can predict the detection probability in areas that have not been investigated.

Figure 5 illustrates the fitted AEPsych models for Study 1 and 2. With the volumetric visualization of the models, we presented the cross section of the models to illustrate more detailed user response trends within 2D trade spaces. The colormap represents the artifact detection probability analyzed by the model and three different contours are given for the detection probabilities of 25%, 50%, and 75%. User responses are also plotted on the figure, with a red cross indicating 'no' and a blue cross indicating 'yes' to the question of "artifact detected?". The response data for the 3D space was projected and flattened to the closest cross-section plane for the illustration.

5.1 Saccadic Suppression

As shown in Fig. 5(a), the artifact detection probability could be less than 50% for <15° saccade amplitude even with the latency of 45 ms. It is the most significant and invaluable finding of our study, as this result supports the existence of a significant contribution from the saccadic suppression. If there is no contribution of saccadic suppression, the latency requirement would be less than ~6 ms [Ratnam et al. 2019] when the marginal pupil size (i.e., exit-pupil diameter subtracted by eye-pupil diameter) is -1 mm. On the other hand, our user study results indicate that we may target much more relaxed requirements. This is a promising sign for SRP development as we may assume that a seamless viewing experience can be achieved with a realistic latency for the pupil steering system. Note that the improvement in the latency (less than 45 ms) will even extend more design space for the exit-pupil diameter or pupil steering resolution, which is beneficial in the optical design.

Another notable trend illustrated in Fig. 5(a) is that the detection probability is less dependent on the marginal pupil size than anticipated, and it generally favors a larger exit-pupil diameter. Although the detection probability peak does appear near the zero marginal pupil size as the saccade amplitude increases, the critical zone is noticeably mitigated. This mitigation is beneficial for the SRP system as it expands the applicable user population, given that the viewing experience is less influenced by the varying eye-pupil diameters of users. In supplementary material, we confirmed that the unique energy distribution of the testbed's exit-pupil smoothed the response trend for the critical area where the exit-pupil and eye-pupil diameters are identical. These results suggest that a freeform exit-pupil can be leveraged to accommodate a broad range of user populations with varying eye-pupil diameter.

5.2 Trade Space for Pupil Steering

The most noticeable finding from Study 2 is that there is no significant trade-off relationship between steering resolution and jitter, as shown in Fig. 5(b). We may even observe some complementary contribution of the steering resolution for the 50% detection probability. This result indicates that the discontinuity of pupil steering may hinder a certain amplitude of jitter and decrease the detection probability. The discrete pupil steering mechanic seems to work as a high-pass amplitude filter and suppress the jitter artifacts. This is also a significant and promising finding for SRP development as we may relax the hardware requirements for the steering device or eye-tracker by leveraging this relationship.

Additionally, it is noteworthy that the y-intercept of the user study aligns well with Ratnam et al.'s model [2019]. The y-intercept corresponds to the viewing conditions where eye movement and jitter are minimized, closely resembling a static environment that can be explained by Ratnam et al.'s model. The model derives the artifact detection threshold by calculating the minimum global transmittance for each condition and identifying the conditions where the global transmittance is 97.5%. The minimum global transmittance occurs for the maximum pupil misalignment given by the full width at half maximum of jitter noise, pupil steering resolution, and the latency. We confirmed that Ratnam et al.'s model also suggests a tolerable pupil steering resolution of around 0.2 mm for y-intercept, which is in good agreement of our user study results.

6 DETECTION PROBABILITY MODEL

We confirmed there is a discrepancy between the user responses and the previous theoretical prediction [Ratnam et al. 2019] in Study 1. Here, we introduce a novel pipeline to predict the detection probability using a temporal frequency analysis of global luminance. The proposed model considers temporal contrast sensitivity, saccadic suppression, and non-linear response of human visual system.

6.1 Hypothesis

There are several hypotheses to derive the theoretical model for the detection probability. First, we assume that artifact detection is mainly involved by temporal modulation of global luminance [Roufs 1972; Watson 1986] across the field of view. The global luminance (L) of the observation imagery is modulated by the pupil alignment errors given by

$$L(t) = L_o * \mathbf{A}(\vec{d}(t), r_{eye}, r_{exit}), \tag{1}$$

where L_o is the baseline luminance (50 cd/m2) of the testbed, and $\mathbf{A}$ is a proportional rate of photons passing through the eye-pupil radius of r_{eye} when the exit-pupil radius of r_{exit} is misaligned by $\vec{d}(t)$. For the eye-pupil, we applied an apodization function considering Stiles-Crawford effect [Westheimer 2008], and the exit-pupil's energy distribution follows as a Gaussian function where the radius is the full width at half maximum. We can derive the pupil misalignment vector using the testbed specification.

$$\vec{d}(t) = \vec{p}_{eye}(t) - \mathbf{R}(\vec{p}_{eye}(t-l) + \vec{j}(t); \Delta t, \Delta x), \tag{2}$$

where $\vec{p}_{eye}$ is the eye-pupil location, $\mathbf{R}$ is a refresh function to discretize the exit-pupil position considering the display refresh interval of Δt and the pupil steering interval of Δx, l is the latency of the pupil steering, and $\vec{j}$ is the Gaussian noise given by the eye-tracking system's jitter.

The second hypothesis is that the visual stimuli will be proportional to the Minkowski summation [To et al. 2011] of the subthreshold component for the luminance change [Tursun and Didyk 2022]. The temporal subthreshold is given by the multiplication of the Fourier transform (**F**) of the global luminance and the temporal contrast sensitivity function.

$$S(f_t) = \mathbf{F}(L(t)) * TCSF(f_t), \tag{3}$$

where $S(f_t)$ is the temporal subthreshold component at frequency of f_t, and $TCSF(f_t)$ is the temporal contrast sensitivity function. Minkowski summation of the temporal subthreshold is

$$C = \left(\sum_{f_t > 0} |S(f_t)|^m \right)^{1/m}, \tag{4}$$

where C is the visual stimulus level, m is the Minkowski coefficient, and we integrate the temporal components for $f_t > 0$ to neglect the DC component.

Finally, we can derive the detection probability model using Weibull psychometric function [Wichmann and Hill 2001], and we introduce another hypothesis to this model. We imitate the saccadic suppression in the model by applying variable parameter for the slope coefficient (α and β) of the psychometric function as follows.

$$P(detection; C) = 1 - \exp\left(-(C/\alpha(v))^{\beta}\right), \tag{5}$$

where the threshold coefficient $\alpha(v)$ is dependent to the saccade amplitude of v as follows.

$$\alpha(v) = \alpha_o * \left(k_0 + (1 - k_0) * \exp\left(-(v/v_0)^{\gamma}\right)\right), \tag{6}$$

where α_o is a coefficient for the detection probability slope, and k_0 represents the maximum saccadic suppression. v_0 and γ determine the slope of the saccadic suppression to the saccade amplitude. Note that this threshold coefficient model was empirically designed to fit with the user study results.

6.2 Model Calibration

The designed model was calibrated with the user study data in Study 1 and 2. As the baseline luminance of the testbed was 50 cd/m^2, and the eye-pupil diameter was fixed to 4 mm [Guillon et al. 2016; Watson and Yellott 2012]. The temporal contrast sensitivity function was derived by the stelaCSF model with the input of corresponding the field of view (50°) and the luminance [Mantiuk et al. 2022]. The saccadic movement of eye-pupil was simulated using a parametric model introduced by Dai et al. [2016] where the $\eta = 400$ and $c = 6$ for the model. The Minkowski coefficient, m, was set to 3 with the given guideline in the previous research [To et al. 2011]. Remained unknown parameters were calibrated by following orders. $\alpha_o = 1.7$ and $\beta = 1.2$ were firstly calibrated to fit with the data of Study 2. Saccadic suppression model coefficients ($k_0 = 16.9, v_0 = 6.5$, and $\gamma = 1.7$) were fitted with data of Study 1.

Figure 6 illustrates the calibrated model with the detection probability prediction. The 50% detection threshold derived by user study results of Study 1 and 2 was plotted together with the model in Fig. 6 (a) and (b). It is observed that our model shows a similar trend with the user study results. As shown in Fig. 6 (c), our model enabled much more convincing interpretation of Study 1 result with the consideration of saccadic suppression. Additionally, the relaxed trade-off between jitter and steering resolution could be comprehended with the proposed model. We could evaluate the fit quality of the calibrated model by calculating the root-mean-square error (RMSE) between the estimated probability distribution from the user study and the predicted detection probability from the calibrated model. The RMSE values for Study 1 and Study 2 were 0.066 and 0.13, respectively. In other words, the predictions for detection probabilities by our model could deviate by approximately 6.6% and 13% in Study 1 and Study 2, respectively.

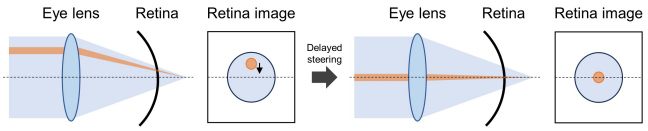

Figure 4: Schematic diagram of the ocular pupil swim involved by aberration of the eye-lens eye. When the exit-pupil is steered within the eye-lens aperture, the ray bundles arrive shifted region if the imaging system has aberration.

7 DISCUSSION

Hardware Requirement for Pupil Steering. This section describes a practice how we can leverage the detection probability model to derive the requirements for an AR SRP system. Firstly, we suppose the eye-pupil diameter is 3 mm, which is average diameter in AR usage environment (>1000 cd/m^2) [Guillon et al. 2016; Watson and Yellott 2012]. Secondly, the exit-pupil is desired to be 2 mm diameter by the diffraction limit requirement for normal vision resolution (60 ppd). Note that the smallest exit-pupil is preferred for a more compact form factor in optical design. Lastly, we predict the pupil steering latency requirement using the detection probability model that we showed in Fig. 6. The desired steering latency for 25% detection probability would be 20 ms for <15° saccade amplitude. Other requirements for pupil steering resolution and jitter can be also referred to the model where the latency is given by 20 ms. The pupil steering resolution and jitter should be less than 0.17 mm and 0.05 mm.

Saccadic Suppression. It is noticeable that saccadic suppression indeed pushes the detection threshold for the pupil steering upward. The detection probability model assumes that saccadic movement suppresses the visual stimuli more than 10 times for the 15 degree saccade amplitude. This level of saccadic suppression was reported in some research papers [Henderson et al. 2008; Stevenson et al. 1986; Uchikawa and Sato 1995], and the suppression level tends to be high for the global luminance change. It gives a significant relaxation for the hardware requirements for SRP system because SRP was thought to be vulnerable to the saccadic movement of eyes. When the eye is static at a point or moves for the smooth pursuit, the pupil misalignment is likely tiny so that it is tolerant without the saccadic suppression.

Ocular Pupil Swim. We conducted pilot surveys to learn which kinds of artifacts are actually observed during the sessions. Our observation was that there is additional visual artifact rather than the global luminance change (flicker). The artifact was occasional

shift of the imagery along with the pupil steering, and it was more clearly observed in Study 2. We found that this artifact, termed ocular pupil swim, is involved by a little shift of the exit-pupil within the aperture of the eye-lens with aberration. Figure 4 illustrates an intuitive example how ray bundles arrive shifted region of the retina when rays pass through a different area of the eye-lens. The figure assumes the vision has the presbyopia where the ocular pupil swim effect is exaggerated. Note that users with normal vision also observes the ocular pupil swim because high-order aberrations [Kang et al. 2010; Nio et al. 2002] also cause the artifact. The maximum ocular swim effect could shift the image approximately 4.5 arcminutes in our testbed, which is near to the detection threshold of 5 arcminutes [Guan et al. 2022]. The more detailed information for the analysis is available in Supplementary Material.

Zero Latency Pupil Steering Testbed. One of the limitations of our testbed is the restricted exploration space for the steering latency. The minimum latency was measured as 45 ms, and we could not further verify the perceptual requirement determined in the previous discussion. In other words, we need to advance or modify the testbed to support the <20 ms latency for further investigation. The testbed demonstrated by P. Guan et al.[2022] could be an option to imitate a near-zero latency eye-tracking system. However, it can only stimulate the vestibulo-ocular reflex, which might yield results overly fitted to this specific eye movement's recognition model. In this study, we rather attempted to leverage an interactive gaze guidance for pseudo eye-tracking without a latency, which is described in Supplementary Material. Although this approach did not work out at this moment, we may polish the study protocol to imitate the ideal eye-tracking system in future work.

8 CONCLUSION

With the development of the SRP perceptual testbed, we have conducted user studies to evaluate the SRP viewing experience and investigate the trade space for the pupil steering parameters. We have also introduced the detection probability model that comprehends the user study results and enabled further understanding how human vision perceives the dynamic pupil steering. The detection probability model allowed us to derive the preliminary perceptual requirements for the AR SRP system. We are hopeful for the SRP development success because the requirements for each parameter are close to the state-of-the-art specifications especially for the eye-tracking system. We believe our study would motivate and inspire several researches to develop low-level hardware components for SRP system.

ACKNOWLEDGMENTS

We would like to extend our gratitude to Aaron Snyder, Rex Li, Greg Petersen, Stephen Choi, Hekun Huang, Nathan Matsuda, Xuan Wang, Olivier Mericer, and Changwon Jang for invaluable support and insightful discussions related to the implementation of the perceptual testbed and the execution of perceptual studies.

REFERENCES

Avi M. Aizenman, George A. Koulieris, Agostino Gibaldi, Vibhor Sehgal, Dennis M. Levi, and Martin S. Banks. 2023. The Statistics of Eye Movements and Binocular Disparities during VR Gaming: Implications for Headset Design. *ACM Trans. Graph.* 42, 1, Article 7 (jan 2023), 15 pages. https://doi.org/10.1145/3549529

Arthur Bradley, Larry Thibos, and David Still. 1990. Visual Acuity Measured with Clinical Maxwellian-View Systems: Effects of Beam Entry Location. *Optometry and Vision Science* 67, 11 (1990), 811–817. https://journals.lww.com/optvissci/fulltext/1990/11000/visual_acuity_measured_with_clinical.4.aspx

Doris I Braun, Alexander C Schütz, and Karl R Gegenfurtner. 2017. Visual sensitivity for luminance and chromatic stimuli during the execution of smooth pursuit and saccadic eye movements. *Vision Research* 136 (2017), 57–69.

Shaoyu Chen, Budmonde Duinkharjav, Xin Sun, Li-Yi Wei, Stefano Petrangeli, Jose Echevarria, Claudio Silva, and Qi Sun. 2022. Instant Reality: Gaze-Contingent Perceptual Optimization for 3D Virtual Reality Streaming. *IEEE Transactions on Visualization and Computer Graphics* 28, 5 (2022), 2157–2167. https://doi.org/10.1109/TVCG.2022.3150522

Steven A. Cholewiak, Zeynep Başgöze, Ozan Cakmakci, David M. Hoffman, and Emily A. Cooper. 2020. A perceptual eyebox for near-eye displays. *Opt. Express* 28, 25 (Dec 2020), 38008–38028. https://doi.org/10.1364/OE.408404

Weiwei Dai, Ivan Selesnick, John-Ross Rizzo, Janet Rucker, and Todd Hudson. 2016. A parametric model for saccadic eye movement. In *2016 IEEE Signal Processing in Medicine and Biology Symposium (SPMB)*. IEEE, Philadelphia, PA, USA, 1–6.

Budmonde Duinkharjav, Praneeth Chakravarthula, Rachel Brown, Anjul Patney, and Qi Sun. 2022a. Image Features Influence Reaction Time: A Learned Probabilistic Perceptual Model for Saccade Latency. *ACM Trans. Graph.* 41, 4, Article 144 (jul 2022), 15 pages. https://doi.org/10.1145/3528223.3530055

Budmonde Duinkharjav, Kenneth Chen, Abhishek Tyagi, Jiayi He, Yuhao Zhu, and Qi Sun. 2022b. Color-Perception-Guided Display Power Reduction for Virtual Reality. *ACM Trans. Graph.* 41, 6, Article 210 (nov 2022), 16 pages. https://doi.org/10.1145/3550454.3555473

Budmonde Duinkharjav, Benjamin Liang, Anjul Patney, Rachel Brown, and Qi Sun. 2023. The Shortest Route is Not Always the Fastest: Probability-Modeled Stereoscopic Eye Movement Completion Time in VR. *ACM Trans. Graph.* 42, 6, Article 220 (dec 2023), 14 pages. https://doi.org/10.1145/3618334

Phillip Guan, Olivier Mercier, Michael Shvartsman, and Douglas Lanman. 2022. Perceptual Requirements for Eye-Tracked Distortion Correction in VR. In *ACM SIGGRAPH 2022 Conference Proceedings* (Vancouver, BC, Canada) *(SIGGRAPH '22)*. Association for Computing Machinery, New York, NY, USA, Article 51, 8 pages. https://doi.org/10.1145/3528233.3530699

Michel Guillon, Kathryn Dumbleton, Panagiotis Theodoratos, Marine Gobbe, C Benjamin Wooley, and Kurt Moody. 2016. The effects of age, refractive status, and luminance on pupil size. *Optometry and vision science* 93, 9 (2016), 1093.

John M Henderson, James R Brockmole, and Daniel A Gajewski. 2008. Differential detection of global luminance and contrast changes across saccades and flickers during active scene perception. *Vision Research* 48, 1 (2008), 16–29.

David M. Hoffman, Ahna R. Girshick, Kurt Akeley, and Martin S. Banks. 2008. Vergence–accommodation conflicts hinder visual performance and cause visual fatigue. *Journal of Vision* 8, 3 (03 2008), 33–33. https://doi.org/10.1167/8.3.33

Saad Idrees, Matthias P. Baumann, Felix Franke, Thomas A. Münch, and Ziad M. Hafed. 2020. Perceptual saccadic suppression starts in the retina. *Nature Communications* 11, 1 (24 Apr 2020), 1977. https://doi.org/10.1038/s41467-020-15890-w

Changwon Jang, Kiseung Bang, Gang Li, and Byoungho Lee. 2018. Holographic Near-Eye Display with Expanded Eye-Box. *ACM Trans. Graph.* 37, 6, Article 195 (dec 2018), 14 pages. https://doi.org/10.1145/3272127.3275069

Changwon Jang, Kiseung Bang, Seokil Moon, Jonghyun Kim, Seungjae Lee, and Byoungho Lee. 2017. Retinal 3D: Augmented Reality near-Eye Display via Pupil-Tracked Light Field Projection on Retina. *ACM Trans. Graph.* 36, 6, Article 190 (nov 2017), 13 pages. https://doi.org/10.1145/3130800.3130889

Pauline Kang, Paul Gifford, Philomena McNamara, Jenny Wu, Stephanie Yeo, Bonney Vong, and Helen Swarbrick. 2010. Peripheral Refraction in Different Ethnicities. *Investigative Ophthalmology & Visual Science* 51, 11 (11 2010), 6059–6065. https://doi.org/10.1167/iovs.09-4747

D. H. Kelly. 1979. Motion and vision. I. Stabilized images of stationary gratings. *J. Opt. Soc. Am.* 69, 9 (Sep 1979), 1266–1274. https://doi.org/10.1364/JOSA.69.001266

Jonghyun Kim, Manu Gopakumar, Suyeon Choi, Yifan Peng, Ward Lopes, and Gordon Wetzstein. 2022. Holographic Glasses for Virtual Reality. In *ACM SIGGRAPH 2022 Conference Proceedings* (Vancouver, BC, Canada) *(SIGGRAPH '22)*. Association for Computing Machinery, New York, NY, USA, Article 33, 9 pages. https://doi.org/10.1145/3528233.3530739

Jonghyun Kim, Youngmo Jeong, Michael Stengel, Kaan Akşit, Rachel Albert, Ben Boudaoud, Trey Greer, Joohwan Kim, Ward Lopes, Zander Majercik, Peter Shirley, Josef Spjut, Morgan McGuire, and David Luebke. 2019. Foveated AR: Dynamically-Foveated Augmented Reality Display. *ACM Trans. Graph.* 38, 4, Article 99 (jul 2019), 15 pages. https://doi.org/10.1145/3306346.3322987

Seong-Bok Kim and Jae-Hyeung Park. 2018. Optical see-through Maxwellian near-to-eye display with an enlarged eyebox. *Opt. Lett.* 43, 4 (Feb 2018), 767–770. https://doi.org/10.1364/OL.43.000767

Joel S. Kollin and Michael R. Tidwell. 1995. Optical engineering challenges of the virtual retinal display. In *Novel Optical Systems Design and Optimization*, Jose M. Sasian (Ed.), Vol. 2537. International Society for Optics and Photonics, SPIE, San Diego, CA, United States, 48 – 60. https://doi.org/10.1117/12.216403

Robert Konrad, Nitish Padmanaban, Keenan Molner, Emily A. Cooper, and Gordon Wetzstein. 2017. Accommodation-Invariant Computational near-Eye Displays. *ACM Trans. Graph.* 36, 4, Article 88 (jul 2017), 12 pages. https://doi.org/10.1145/3072959.3073594

Brooke Krajancich, Petr Kellnhofer, and Gordon Wetzstein. 2021. A Perceptual Model for Eccentricity-Dependent Spatio-Temporal Flicker Fusion and Its Applications to Foveated Graphics. *ACM Trans. Graph.* 40, 4, Article 47 (jul 2021), 11 pages. https://doi.org/10.1145/3450626.3459784

Gregory Kramida. 2016. Resolving the Vergence-Accommodation Conflict in Head-Mounted Displays. *IEEE Transactions on Visualization and Computer Graphics* 22, 7 (2016), 1912–1931. https://doi.org/10.1109/TVCG.2015.2473855

John Krauskopf. 1980. Discrimination and detection of changes in luminance. *Vision Research* 20, 8 (1980), 671–677. https://doi.org/10.1016/0042-6989(80)90091-7

Seungjae Lee, Mengfei Wang, Gang Li, Lu Lu, Yusufu Sulai, Changwon Jang, and Barry Silverstein. 2020. Foveated near-eye display for mixed reality using liquid crystal photonics. *Scientific Reports* 10, 1 (30 Sep 2020), 16127. https://doi.org/10.1038/s41598-020-72555-w

Robert LiKamWa, Zhen Wang, Aaron Carroll, Felix Xiaozhu Lin, and Lin Zhong. 2014. Draining our glass: an energy and heat characterization of Google Glass. In *Proceedings of 5th Asia-Pacific Workshop on Systems* (Beijing, China) *(APSys '14)*. Association for Computing Machinery, New York, NY, USA, Article 10, 7 pages. https://doi.org/10.1145/2637166.2637230

Junguo Lin, Dewen Cheng, Cheng Yao, and Yongtian Wang. 2017a. Retinal projection head-mounted display. *Frontiers of Optoelectronics* 10, 1 (01 Mar 2017), 1–8. https://doi.org/10.1007/s12200-016-0662-8

Junguo Lin, Dewen Cheng, Cheng Yao, and Yongtian Wang. 2017b. Retinal projection head-mounted display. *Frontiers of Optoelectronics* 10 (2017), 1–8.

Tiegang Lin, Tao Zhan, Junyu Zou, Fan Fan, and Shin-Tson Wu. 2020. Maxwellian near-eye display with an expanded eyebox. *Opt. Express* 28, 26 (Dec 2020), 38616–38625. https://doi.org/10.1364/OE.413471

Rafał K. Mantiuk, Maliha Ashraf, and Alexandre Chapiro. 2022. StelaCSF: A Unified Model of Contrast Sensitivity as the Function of Spatio-Temporal Frequency, Eccentricity, Luminance and Area. *ACM Trans. Graph.* 41, 4, Article 145 (jul 2022), 16 pages. https://doi.org/10.1145/3528223.3530115

Ethel Matin. 1974. Saccadic suppression: A review and an analysis. *Psychological Bulletin* 81, 12 (1974), 899 – 917.

Y. K. Nio, N. M. Jansonius, V. Fidler, E. Geraghty, S. Norrby, and A. C. Kooijman. 2002. Spherical and irregular aberrations are important for the optimal performance of the human eye. *Ophthalmic and Physiological Optics* 22, 2 (2002), 103–112. https://doi.org/10.1046/j.1475-1313.2002.00019.x

Lucy Owen, Jonathan Browder, Benjamin Letham, Gideon Stocek, Chase Tymms, and Michael Shvartsman. 2021. Adaptive Nonparametric Psychophysics. arXiv:2104.09549 [stat.ME]

Anjul Patney, Marco Salvi, Joohwan Kim, Anton Kaplanyan, Chris Wyman, Nir Benty, David Luebke, and Aaron Lefohn. 2016. Towards Foveated Rendering for Gaze-Tracked Virtual Reality. *ACM Trans. Graph.* 35, 6, Article 179 (dec 2016), 12 pages. https://doi.org/10.1145/2980179.2980246

Dale Purves and Stephen Mark Williams. 2001. *Neuroscience. 2nd edition.* Sinauer Associates 2001. http://lib.ugent.be/catalog/ebk01:3450000000002013

Kavitha Ratnam, Robert Konrad, Douglas Lanman, and Marina Zannoli. 2019. Retinal image quality in near-eye pupil-steered systems. *Opt. Express* 27, 26 (Dec 2019), 38289–38311. https://doi.org/10.1364/OE.27.038289

John G Robson. 1966. Spatial and temporal contrast-sensitivity functions of the visual system. *Josa* 56, 8 (1966), 1141–1142.

JAJ Roufs. 1972. Dynamic properties of vision—II. Theoretical relationships between flicker and flash thresholds. *Vision Research* 12, 2 (1972), 279–292.

Weitao Song, Xinan Liang, Shiqiang Li, Parikshit Moitra, Xuewu Xu, Emmanuel Lassalle, Yuanjin Zheng, Yongtian Wang, Ramón Paniagua-Domínguez, and Arseniy I Kuznetsov. 2023. Retinal Projection Near-Eye Displays with Huygens' Metasurfaces. *Advanced Optical Materials* 11, 5 (2023), 2202348.

S.B. Stevenson, F.C. Volkmann, J.P. Kelly, and L.A. Riggs. 1986. Dependence of visual suppression on the amplitudes of saccades and blinks. *Vision Research* 26, 11 (1986), 1815–1824. https://doi.org/10.1016/0042-6989(86)90133-1

Larry N. Thibos, Ming Ye, Xiaoxiao Zhang, and Arthur Bradley. 1992. The chromatic eye: a new reduced-eye model of ocular chromatic aberration in humans. *Appl. Opt.* 31, 19 (Jul 1992), 3594–3600. https://doi.org/10.1364/AO.31.003594

MPS To, Roland J Baddeley, T Troscianko, and DJ Tolhurst. 2011. A general rule for sensory cue summation: Evidence from photographic, musical, phonetic and cross-modal stimuli. *Proceedings of the Royal Society B: Biological Sciences* 278, 1710 (2011), 1365–1372.

Cara Tursun and Piotr Didyk. 2022. Perceptual Visibility Model for Temporal Contrast Changes in Periphery. *ACM Trans. Graph.* 42, 2, Article 20 (nov 2022), 16 pages. https://doi.org/10.1145/3564241

Keiji Uchikawa and Masayuki Sato. 1995. Saccadic suppression of achromatic and chromatic responses measured by increment-threshold spectral sensitivity. *JOSA A* 12, 4 (1995), 661–666.

A. Van Meeteren and C.J.W. Dunnewold. 1983. Image quality of the human eye for eccentric entrance pupils. *Vision Research* 23, 5 (1983), 573–579. https://doi.org/10.1016/0042-6989(83)90133-5

Andrew Watson. 1986. Temporal Sensitivity. *Handbook of perception and human performance* 1, 6 (02 1986), 1–43.

Andrew B. Watson and John I. Yellott. 2012. A unified formula for light-adapted pupil size. *Journal of Vision* 12, 10 (09 2012), 12–12. https://doi.org/10.1167/12.10.12

Gerald Westheimer. 1966. The maxwellian view. *Vision Research* 6, 11 (1966), 669–682. https://doi.org/10.1016/0042-6989(66)90078-2

Gerald Westheimer. 2008. Directional sensitivity of the retina: 75 years of Stiles–Crawford effect. *Proceedings of the Royal Society B: Biological Sciences* 275, 1653 (2008), 2777–2786. https://doi.org/10.1098/rspb.2008.0712

Felix A Wichmann and N Jeremy Hill. 2001. The psychometric function: I. Fitting, sampling, and goodness of fit. *Perception & psychophysics* 63, 8 (2001), 1293–1313.

Jianghao Xiong, Yannanqi Li, Kun Li, and Shin-Tson Wu. 2021. Aberration-free pupil steerable Maxwellian display for augmented reality with cholesteric liquid crystal holographic lenses. *Opt. Lett.* 46, 7 (Apr 2021), 1760–1763. https://doi.org/10.1364/OL.422559

Chenchen Zhang, Dewen Cheng, Junguo Lin, and Yongtian Wang. 2020. Retinal projection display system based on MEMS scanning projector and conicoid curved semi-reflective mirror. In *AOPC 2020: Display Technology; Photonic MEMS, THz MEMS, and Metamaterials; and AI in Optics and Photonics*, Vol. 11565. SPIE, Beijing, China, 20–25.

Junyu Zou, Lingshan Li, and Shin-Tson Wu. 2022. Gaze-Matched Pupil Steering Maxwellian-View Augmented Reality Display with Large Angle Diffractive Liquid Crystal Lenses. *Advanced Photonics Research* 3, 5 (2022), 2100362. https://doi.org/10.1002/adpr.202100362

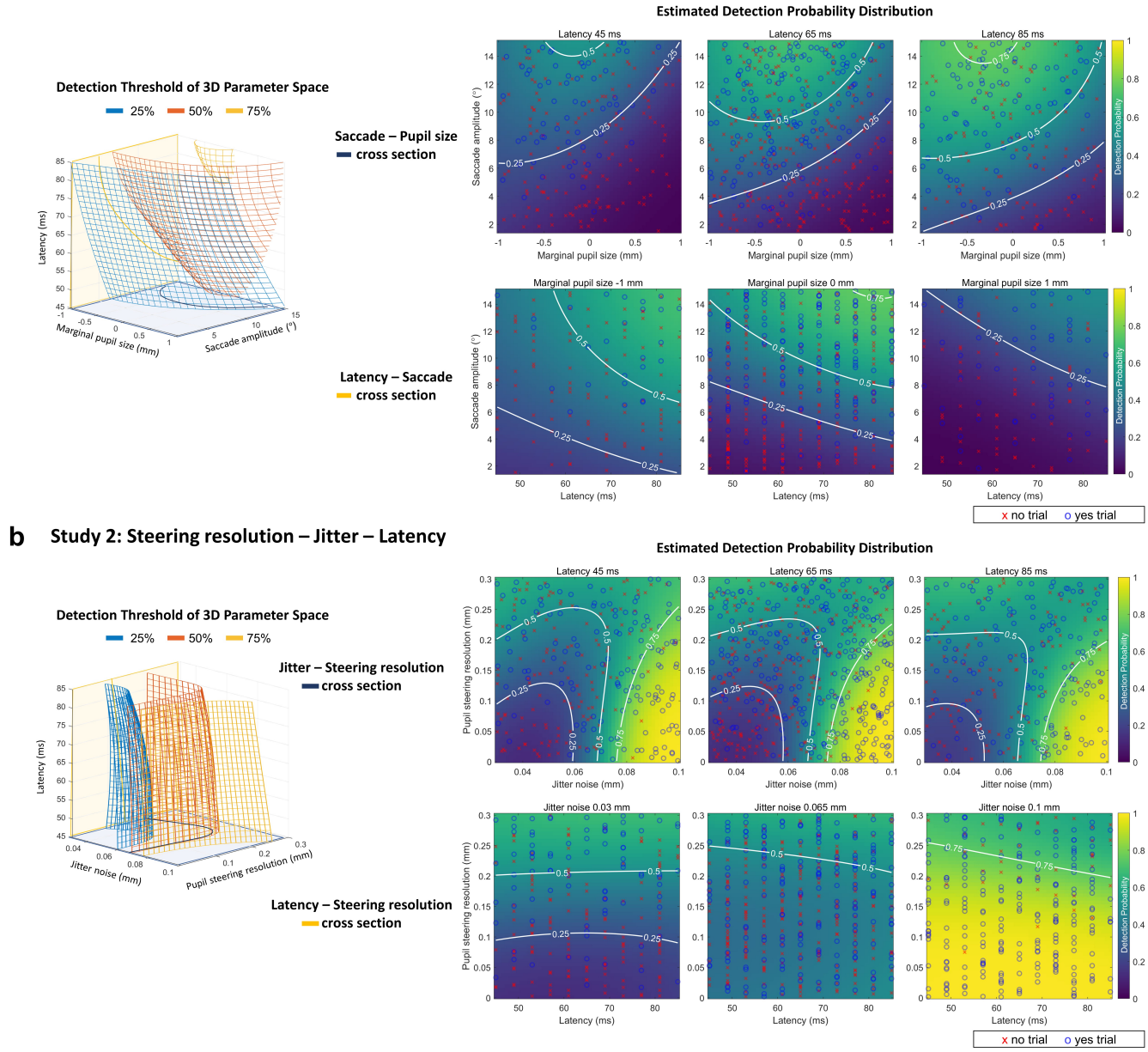

Figure 5: User study results for (a) Study 1 and (b) Study 2. Each study was conducted to explore different 3D trade space: saccade amplitude - marginal pupil size - latency, and steering resolution - jitter - latency, respectively. (a) Study 1 aims to analyze the effect of the saccadic suppression to the SRP viewing experience. (b) Study 2 aims to explore the trade space among pupil steering parameters for SRP viewing experience. The user responses for the query of "artifact detected?" were recorded as 'yes' or 'no', and each trial marked as circle or cross in the figure. On the right hand, we illustrated the 2D sliced images for the detection probability along the latency axis. The 2D sliced image is given by the perpendicular projection of 3D data to the closest plane.

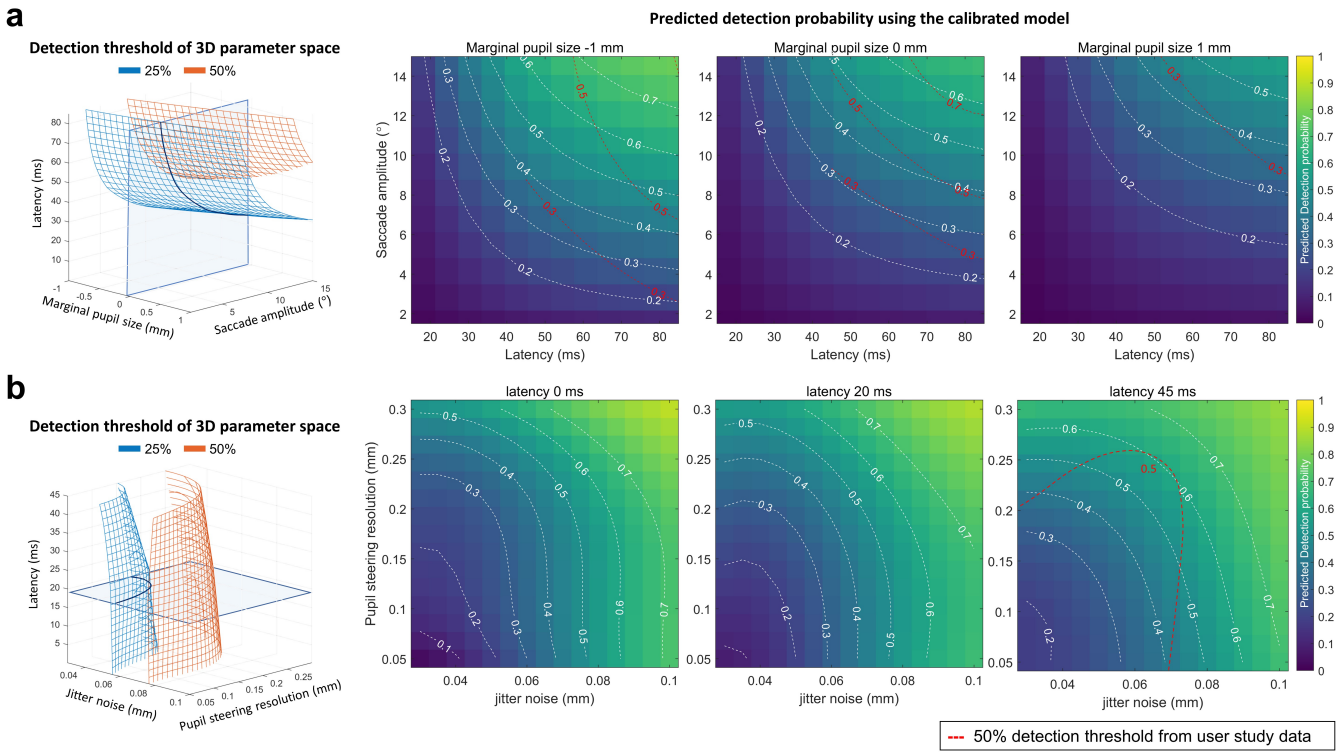

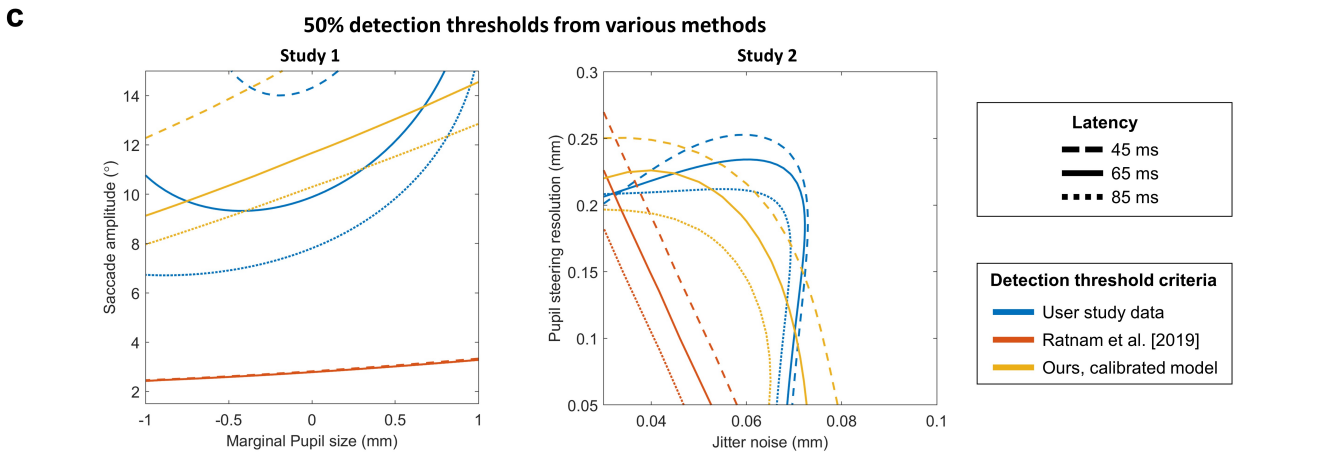

Figure 6: (a-b) Analysis of 3D trade space for pupil steering parameters using the proposed detection probability model. The white lined contours represent our model's prediction and the red dot lines are plotted by the AEPsych models fitted for Study 1 or 2 results. We illustrated the proposed model's prediction on the trade space designed for (a) Study 1 and (b) Study 2. As illustrated in the figures, our model allows us to investigate the extended trade space where the tested could not reproduce. We may also roughly estimate the perceptual requirements for steering devices and eye-tracking systems. (c) To evaluate the fitting quality of our model, we illustrate and compare 50% detection threshold given by three different models: AEPsych model derived from the user study data, the global transmission analysis model proposed by Ratnam et al. [2019], and our calibrated model. These three models' prediction are illustrated by different colored lines, and three different latencies (45 ms, 65 ms, 85 ms) are represented by the line style. Our calibrated model exhibits an enhanced capability in the detection probability prediction over the method employed by Ratnam et al. [2019]. For quantitative comparison, we calculated the RMSE values at the 50% detection threshold considering the approach of Ratnam et al. [2019] only obtains the detection threshold without the detection probability prediction across the parameter space. The RMSE values for our model were 0.071 and 0.083 for Study 1 and Study 2, respectively. In comparison, Ratnam et al.'s model yielded RMSE values of 0.38 and 0.19.